HEAT and TECHNOLOGY
CALORE e TECNOLOGIA
Vol. 6 • No. 1-2 • 1988

ANISOTROPIC TURBULENT TRANSPORT MODELING FOR ROD-BUNDLE

Marcelo J.S. de Lemos (*)

Abstract

It is well known in the literature that eddy-diffusivity turbulence models can only lead to isotropic turbulent coefficients for linking the Reynolds Stresses/Fluxes to the gradients of the mean velocity/temperature. In the particular case of axial flow through rod-bundles, however, transport coefficients for channel faces aligned with rod centers are known to be considerably higher than those calculated by simple isotropic theories. Based on the foregoing application, this work presents an attempted to describe the anisotropy of turbulent transport in rod arrays by means of an Algebraic Stress Model. Results for all three normal components of the Reynolds Stress tensor are presented and compared with experimental data. Predictions show good agreement for the Reynolds number and the range of aspect ratio (Rod pitch/Diameter) investigated.

NOMENCLATURE

c model constants
D rod diameter
f wall effect function
k turbulent kinetic energy, $\overline{u_i u_i}/2$
l turbulence length scale, $k^{3/2}/\epsilon$
P rod pitch; $-\overline{u_i u_j}\,\frac{\delta U_i}{\delta x_j}$ = generation rate of turbulence energy due to mean velocity gradients

P_{ij} kinematic production rate of $\overline{u_i u_j}$ by mean velocity gradients; $-\left[\overline{u_i u_k}\,\frac{\delta U_j}{\delta x_k} + \overline{u_j u_k}\,\frac{\delta U_i}{\delta x_k}\right]$

Re Reynolds number
U_z mean velocity in the mean direction
u_i fluctuating velocity component in i direction, i=r,θ,z

$\overline{u_i u_j}$ kinematic Reynolds Stress
y distance from rod wall

(*) Department of Energy, IEME/ITA/CTA, Sao José dos Campos, Sao Paulo 12225, Brasil.

$\hat{y}$ distance from rod wall to maximum velocity line
$\hat{y}^*$ maximum value for $\hat{y}$, correspondent to θ^*

Greek Symbols

ϵ kinematic dissipation rate of turbulent kinetic energy
θ angular coordinate
θ^* maximum value for θ; $\theta^*=45°$ for square lattice, $\theta^*=30°$ for triangular array
π_{ij} pressure-strain correlation (general),

$$\overline{\frac{p}{\rho}\left[\frac{\delta u_i}{\delta x_j}+\frac{\delta u_j}{\delta x_i}\right]}$$

$\pi_{ij,1}$ first part of π_{ij}, associated with turbulence-velocity interactions

$$-c_1\frac{\epsilon}{k}\left[\overline{u_i u_j}-\frac{2}{3}\delta_{ij}k\right]$$

$\pi_{ij,2}$ second part of π_{ij}, associated with turbulence-velocity interactions

$$-c_2\left[P_{ij}-\frac{2}{3}\delta_{ij}P\right]$$

INTRODUCTION

In axial flow through rod-bundles, transport coefficients for cell faces aligned with rod centers are known to be considerably higher than those calculated by simple isotropic theories. In this category it is also included the widely-used k-ϵ model. And yet, it has been found that secondary flows play only a minor role in this overall transport, being turbulence highly enhanced across that hypothetical surface [1-4]. Enhancement of that particular mechanism is due to the intriguing fact that when two adjacent subchannels have the "gap" between them reduced, for instance by closely packing the pins, the total transport across that surface is nearly constant. At a first glance, one would expect that the closer the rods, the higher the resistance to any mechanism of exchange between channels.

In order to calculate the correct amount of the quantity being transported, the approach taken by many investigators was then to artificially increase the diffusion coefficient obtained via a simpler isotropic theory (usually the standard k-ϵ model) and numerically "match" the experimentally observed mixing rates. Solutions of this kind are presented in Refs. 2 and 3. These approaches clearly identify the need for a better understanding of the mixing phenomena taking place in that geometry.

Based on the foregoing application, the present author, in an early work [5], attempted to describe the enhancement of turbulence across subchannel boundaries through the modeling of the normal Reynolds Stresses. An Algebraic Stress Model (ASM) based on the assumption of local equilibrium for turbulence (Production = Dissipation) was used. The ASM involves an

approximation of the full transport equations for $-\overline{u_i u_j}$ and carry along all significant information on the several processes contributing to the total level of $-\overline{u_i u_j}$.

The present work extend those modeling ideas and reports predictions for the energy exchange among stresses without the local equilibrium restriction. The following sections present a model for turbulent normal stresses as well as numerical results and comparison with experimental data.

A MODEL FOR THE REYNOLDS STRESSES

The concept of subchannel is often used in the literature in connection with nuclear reactor thermal-hydraulic analysis. Typical subchannels for triangular and square arrays are schematically shown in Fig. 1. It is emphasized that the class of problems here studied is that associated with fully developed situations. So no shear stresses are considered on the r-θ plane, since inclusion of these stresses would preclude the neglecting of diffusion transport along the streamwise direction.

The complete full transport equation for the stresses $-\overline{u_i u_j}$ can be transformed into a more simple, easy-to-handle, algebraic equation by means of the well-known approximation proposed by Rodi[6]

$$\overline{u_i u_j} = k\left[\frac{2}{3}\delta_{ij} + \frac{(1-c_2)\frac{P_{ij}}{\epsilon} - \frac{2}{3}\delta_{ij}\frac{P}{\epsilon} + \frac{\pi_{ij,w}}{\epsilon}}{c_1 + \frac{P}{\epsilon} - 1}\right] \tag{1}$$

where k is the turbulent kinetic energy per unit mass, and gravitational effects are neglected. The quantities P_{ij} and P represent the production rates of $-\overline{u_i u_j}$ and k due to the mean velocity gradients, respectively. The correlation $\pi_{ij,w}$ is a correction applied to the "pressure-strain" term π_{ij}, to indicate the effect of nearby walls on the fluctuating pressure field p. When Eq. 1 is written for the cylindrical coordinate system in Fig. 1, the five important stresses are then:

$$\overline{u_z u_r} = \frac{k}{\epsilon}\left[(c_1-1) + \frac{P}{\epsilon}\right]^{-1}\left[-\overline{u_r^2}\frac{\delta U_z}{\delta r}(1-c_2) + \pi_{rz,w}\right] \tag{2}$$

$$\overline{u_z u_\theta} = \frac{k}{\epsilon}\left[(c_1-1) + \frac{P}{\epsilon}\right]^{-1}\left[-\overline{u_\theta^2}\frac{\delta U_z}{r\delta\theta}(1-c_2) + \pi_{\theta z,w}\right] \tag{3}$$

$$\overline{u_r^2} = \frac{k}{\epsilon}\left[(c_1-1) + \frac{P}{\epsilon}\right]^{-1}\left[\frac{2}{3}c_2 P + \pi_{rr,w} + \frac{2}{3}(c_1-1)\epsilon\right] \tag{4}$$

$$\overline{u_\theta^2} = \frac{k}{\epsilon}\left[(c_1-1) + \frac{P}{\epsilon}\right]^{-1}\left[\frac{2}{3}c_2 P + \pi_{\theta\theta,w} + \frac{2}{3}(c_1-1)\epsilon\right] \tag{5}$$

$$\overline{u_z^2} = \frac{k}{\epsilon}\left[(c_1-1)+\frac{P}{\epsilon}\right]^{-1}\left[\frac{2}{3}(3-2c_2)P + \pi_{zz,w} + \frac{2}{3}(c_1-1)\epsilon\right] \tag{6}$$

where

$$P = -\overline{u_z u_r}\,\frac{\delta U_z}{\delta r} - \overline{u_z u_\theta}\,\frac{\delta U_z}{r\delta\theta} \tag{7}$$

In the above equations, ϵ is the dissipation rate of k, c's are constants and π's are components of $\pi_{ij,w}$.

Proposal for $\pi_{ij,w}$

The wall correction to $\pi_{ij,w}$ has its origin in the integration of a Poisson equation for the fluctuating pressure p, over a surface-bounded field. The surface integral part of the resulting expression can then be multiplied by the fluctuating strain-field, and, after time-averaging, it yields $\pi_{ij,w}$ [7]. The physical significance of $\pi_{ij,w}$ is therefore the overall effect that a surface (a rigid wall or a free surface) has upon π_{ij}.

An expression for $\pi_{ij,w}$ was first suggested by Shir[8], and has been used for rod arrays by deLemos [5], giving for the several components;

$$\pi_{zr,w} = -c_1'\frac{\epsilon}{k}\overline{u_z u_r}\,\frac{3}{2}f - c_2c_2'\,\overline{u_r^2}\,\frac{\delta U_z}{\delta r}\,\frac{3}{2}f \tag{8}$$

$$\pi_{z\theta,w} = 0 \tag{9}$$

$$\pi_{rr,w} = -2\,\frac{\epsilon}{k}\,c_1'\,\overline{u_r^2}\,f - \frac{4}{3}\,c_2c_2'f\,P \tag{10}$$

$$\pi_{\theta\theta,w} = \frac{\epsilon}{k}\,c_1'\,\overline{u_r^2}\,f + \frac{2}{3}\,c_2c_2'f\,P \tag{11}$$

and

$$\pi_{zz,w} = \frac{\epsilon}{k}\,c_1'\,\overline{u_r^2}\,f + \frac{2}{3}\,c_2c_2'f\,P \tag{12}$$

It is noticed that

$$\pi_{rr,w} = -2\,\pi_{\theta\theta,w} = -2\,\pi_{zz,w}$$

and that under contraction of indexes, $\pi_{ii,w}=0$, as expected. After substituting Eqs. 10 through 12 back into Eqs. 4 through 6, the normal stresses are then given by:

$$\frac{\overline{u_r^2}}{k} = \frac{2}{3}\left[\frac{\frac{P}{\epsilon}\,c_2\,(1-2c_2'f)+c_1-1}{c_1+2c_1'f+\frac{P}{\epsilon}-1}\right] \tag{13}$$

$$\frac{\overline{u_\theta^2}}{k} = \frac{2}{3} + \left[\frac{(c_2 - 1)\frac{2}{3}\frac{P}{\epsilon} + c_1' \frac{\overline{u_r^2}}{k} f + \frac{2}{3} c_2 c_2' f \frac{P}{\epsilon}}{c_1 + \frac{P}{\epsilon} - 1} \right] \tag{14}$$

and

$$\frac{\overline{u_z^2}}{k} = \frac{2}{3} + \left[\frac{(1 - c_2)\frac{4}{3}\frac{P}{\epsilon} + c_1' \frac{\overline{u_r^2}}{k} f + \frac{2}{3} c_2 c_2' f \frac{P}{\epsilon}}{c_1} \right] \tag{15}$$

From Eqs. 2 and 3, with assumptions os Eqs. 8 and 9, the ratio of shear stress is given by

$$\frac{\overline{u_z u_\theta}}{\overline{u_z u_r}} = K \frac{\overline{u_\theta^2}}{\overline{u_r^2}} \frac{\frac{\delta U_z}{r\delta\theta}}{\frac{\delta U}{\delta r}} \tag{16}$$

where

$$K = \frac{c_1 + c_1' \frac{3}{2} f + \frac{P}{\epsilon} - 1}{\left(1 + \frac{3}{2} \frac{c_2 c_2'}{(1 - c_2)} f \right)\left(\frac{P}{\epsilon} + c_1 - 1 \right)} \tag{17}$$

Now, comparing Eq. 16 with the eddy-diffusivity expression, one has;

$$\frac{\mu_{\theta\theta}}{\mu_{rr}} = K \frac{\overline{u_\theta^2}}{\overline{u_r^2}} \tag{18}$$

where $\mu_{\theta\theta}$ and μ_{rr} is a second-order tensor representing the directional turbulent viscosity.

Using Eqs. 4 and 5, the ratio of normal stresses in Eq. 18 can be given

$$\frac{\overline{u_\theta^2}}{\overline{u_r^2}} = \frac{\frac{P}{\epsilon}(c_2 + c_2 c_2' f) + c_1 - 1 + \frac{3}{2} c_1' \frac{\overline{u_r^2}}{k} f}{\frac{P}{\epsilon}(c_2 - 2c_2 c_2' f) + c_1 - 1 - 3 c_1' \frac{\overline{u_r^2}}{k} f} \tag{19}$$

From Eq. 19 one sees that if f = 0, the normal stresses are equal, or say, assuming all simplifications made so far, the differences in the normal stresses are seen to be solely caused by the effect of the subchannel walls on the fluctuating pressure field.

The functional f

Launder et al [9] suggest for "f" a linear relationship of the form

$$f = \frac{l}{c_w x_n} = \frac{k^{3/2}}{c_w \epsilon} \tag{20}$$

where c_w is a constant and "l" a turbulence length scale. Due to difficulties in prescribing the length scale for the geometry in question, the following relationship for f was adopted in Ref. [5]:

$$f = 1 - \left[\frac{y}{y^*}\right]^n \tag{21}$$

where n = 1, and

$$\hat{y}^* = \frac{D}{2}\left[\frac{P}{D\cos\theta^*} - \frac{1}{2}\right] \tag{22}$$

Equation 21 gives f = 1 for y = 0, and f = 0 only at $y = \hat{y}^*$ and $\theta = \theta^*$. This expression is in agreement with the idea that by either way (decreasing θ or P/D) one is getting closer to the wall surface. A discussion on the effect of the exponent "n" is shown in Ref. [5]. In that work, it was found that results for all the three normal stresses are not too sensitive to this function. Yet, it was also reported that f could not represent the exchange of energy between the axial and tangential direction, since variations in f would cause changes in the same direction, for both $\overline{u_\theta^2}/k$ and $\overline{u_z^2}/k$. Nevertheless, the functional f, as presented by Eq. 21, is here included for the sake of completeness.

The functional P/ϵ

Since the full system of equations is not solved in the present work (including equation for k and ϵ), predictions for the normal stresses can only be achieved through the prescription of P/ϵ in the calculation domain. In the present work, the following relationship for P/ϵ is adopted:

$$\frac{P}{\epsilon} = (1 - (y/\hat{y})^{0.5}) - (10.283 - P/D\ 8.597)\ y/\hat{y}\ \theta/\theta^* \tag{23}$$

where P/D is the Pitch-to-diameter ratio (It should be noticed that, for notation simplicity, the same symbol is given for the production rate of turbulent kinetic energy and for the rod pitch, namely P).

The first part of the right-hand-side of (23) express the idea that close to the wall ($y \to 0$) the turbulent energy balance should approach the equilibrium situation ($P=\epsilon$). The second part is a correction applied to the first one, and is a linear fitting to the measured values at the center point ($y = \hat{y}^*$, $\theta = \theta^*$) reported by Hooper[10]. The factors $y/\hat{y}$ and θ/θ^* indicate that this correction dies out as either y or θ approach to zero.

With the prescription of P/ϵ and f, the normal stresses and the ratio of eddy diffusivity coefficients can now be calculated. The following section presents results and comparisons with available experimental data.

RESULTS AND DISCUSSION

The set of algebraic equations 13-15 was calculated with the functions f and P/ϵ described above and the following constants:

$$c_1 = 1.8 \; ; \; c_1' = 0.5 \; ; \; c_2 = 0.6 \text{ and } c_2' = 0.3$$

Predictions were compared with data of Hooper[10] for a square lattice ($\theta^* = 45°$) with Re = 48000 and for two aspect ratios P/D, equal to 1.107 and 1.194, respectively.

Before presenting results for $\overline{u_r^2}/k$, $\overline{u_\theta^2}/k$ and $\overline{u_z^2}/k$, it is interesting to investigate the role of the functions P/ϵ, f, and constant c_2 on the level of the stresses. In addition, it is important to emphasize that it is their combined effect which will count.

Quick hand calculations with the constants given above can readily show that the higher P/ϵ, the higher $\overline{u_z^2}/k$. An opposite trend is obtained for $\overline{u_r^2}/k$ and $\overline{u_\theta^2}/k$. An inspection on the multipliers of P/ϵ in Eqs. (13)-(15) could also have led to the same conclusions. These behaviors may have the physical interpretation that the higher the overall production of energy, the more unequal will be the distribution of it among the stresses. Thus, for a high P/ϵ ratio, $\overline{u_z^2}/k$ will carry relatively more energy than the other two components.

On the other hand, the wall correction added to π_{ij} and represented by Eqs. 10-12 indicates that the amount of energy being damped by the wall in the radial direction is equally divided and fed into the z and θ axes. In addition, c_2 comes from the modeling of the mean-field part of the pressure--strain correlation, or

$$\pi_{ij,2} = - c_2 \left[P_{ij} - \frac{2}{3} \delta_{ij} P \right] \qquad (24)$$

Considering that the present flow is fully dominated by radial and azimuthal gradients of the axial velocity[11], all turbulent energy will be generated in the axial direction and transferred by pressure fluctuations to $\overline{u_r^2}$ and $\overline{u_\theta^2}$. Then the term $\pi_{ij,2}$ will be a sink for $\overline{u_z^2}$ ($P_{zz} = 2P$) and a source for the other two stresses ($P_{rr} = P_{\theta\theta} = 0$). The combined role of P/ϵ, f and c_2 can now be assessed.

In Eq. 13, f will act to reduce c_2., or say, it will act to diminish the transfer of energy to that particular direction. On the other hand, f greater than zero can be seen as increasing c_2 for $\overline{u_\theta^2}$ and $\overline{u_z^2}$, and this can be physically interpreted as an increase in the source terms $\pi_{\theta\theta,2}$ and $\pi_{zz,2}$, respectively. These ideas, together with the sensitivity of P/ϵ commented above, show that an increase in c_2 or a reduction in P/ϵ will induce both similar trends on the relative stress values. It is interesting to point out that this state-of-affairs, together with the local equilibrium assumption (P=ϵ) used in Ref.[5], led the author in that work to suggest that better results for the turbulent normal stresses could be obtained by means of a change in the c_2 value across the domain of calculation.

With these ideas in mind, results for the stresses can now be presented and more clearly discussed.

Figure 2 presents results for P/D = 1.107. The reduction of $\overline{u_r^2}/k$ as the gap region (θ = 0°) approaches is well calculated. Results for $\overline{u_\theta^2}/k$ show that the amount of enhancement at the gap region is only slightly under-predicted. Calculated $\overline{u_z^2}/k$ profiles also show an over-prediction at corresponding locations, probably indicating that the functional "f" should give a greater value in the gap region. It is therefore shown that the substantial enhancement in $\overline{u_\theta^2}/k$ as the gap is approached can only be partially predicted with the model here presented.

Figure 3 presents results for P/D = 1.194. The experimental values for $\overline{u_\theta^2}/k$, $\overline{u_r^2}/k$, and $\overline{u_z^2}/k$ at the center-point ($\theta = \theta_m$, $y = \hat{y}^*$) and at the middle of the gap (θ = 0°, $y = \hat{y}$) was obtained as expected, since Eq. (23) was derived with the help of those same experimental data. In using Eq. (23), however, the curves fall higher than experimental values for $\overline{u_\theta^2}/k$ as the wall is approached. The opposite trend is obsderved for $\overline{u_r^2}/k$. These predictions seem to suggest that a better representation for the distribution of P/ϵ is necessary. Equation (23) should then be regarded as a first approximation, subjected to refinement as more data are gathered. Also important for improving the present calculations is certainly the combined solution of the transport equations for k and ϵ, giving the calculated P/ϵ ratio everywhere in the flow field.

Figure 4 finally shows the calculated profiles for the anisotropy factor $\mu_{\theta\theta}/\mu_{rr}$, for P/D = 1.107. At the line of maximum velocity ($y = \hat{y}$) the increasing ratio as the wall is approached is well predicted. However, due to the sensitivity of the results shown so far on P/ϵ and f, predictions fall below experimental values reported in the literature for the region close to the surface. An anisotropy factor of as much as 5-10 has been reported by Rehme[4] in that region, whereas predictions show a factor of about 2.23. Nevertheless, the present calculations should be regarded as a first approximation as mentioned above, identifying the need for a better modeling of the physical processes involved.

It should be also pointed out that in spite of the difficulties which arose, the model shown in this work represents a step toward reliable turbulence modeling for closely packed rod arrays. In addition, it is certainly a more realistic approach to represent the anisotropy of transport coefficients than to simply prescribe empirical anisotropy factors.

CONCLUDING REMARKS

This paper reported an attempt to describe the anisotropy on the levels of normal turbulent stresses and corresponding effects on the coefficients of turbulent transport for rod arrays. Results for the center region and gap are well calculated with the empirical function P/ϵ. The strong coupling between the axial and lateral stresses at the gap region is well represented, but it is recognized that a true representation of P/ϵ in the subchannel is necessary before any conclusion can be drawn. An analysis of the equations representing the stresses indicates that the effect of changing P/ϵ from unity is numerically similar to varying the constant c_μ in the domain. It was also pointed out that correct redistribution of turbulent

kinetic energy extracted from the mean flow can be obtained by solving the accompanying equations for k and ϵ. Results were considered as a first approximation, subject to future refinement.

ACKNOWLEDGEMENTS

The author wishes to thank CNPq - Conselho Nacional de Desenvolvimento Científico e Tecnológico, Brazil, for supporting this work through grant #30.2276/86-EM.

REFERENCES

1. Seale, W.J., Nuclear Engineering & Design, vol. 54, pp. 197-209 (1979).

2. Bartiz, J., Todreas, N.;Journal of Heat Transfer, to be published.

3. Yang, Chang, Journal of Heat Transfer, to be published.

4. Rehme, K., paper 16-D, Proc. III Topical Meeting on Reactor Thermal Hydraulics, Newport, RI (1985).

5. deLemos, M.J.S.; An Algebraic Stress Model For Axial Flow In a BAre Rod-Bundle, Proc. 2nd ASME/JSME Thermal Eng. Joint Conf., Honolulu, Vol. 1, pp. 461-466 (1987).

6. Rodi, W.,The Prediction of Free Turbulent Boundary Layers by Use of a Two-Equation Model of Turbulence, PhD Thesis, University of London (1972).

7. Chou, P.Y.,On Velocity Correlation and the Solution of the Equations of Turbulent Fluctuations, Quartely Journal Mech. Appl. Math., vol.3, pp. 38 - 54 (1945).

8. Shir, C.C., A Preliminary Numerical Study of Atmospheric Turbulent Flow In the Idealized Boundary Layer, Journal Atmos. Sci., vol. 30, p. 1327 (1973).

9. Launder, B.E., Reece, G.L., and Rodi, W., Progress in the Development of a Reynolds Stress Turbulence Closure, Journal of Fluid Mechanics, vol. 68, pp. 537-566 (1975).

10. Hooper, J.D., Developed Single Phase Turbulent Flow Through a Square--Pitch Rod Cluster, Nuclear Eng. & Design, vol. 60, pp. 365-379 (1980).

11. Hooper, J.D., and Wood. D.H., Fully Developed Rod Bundle Flow Over a Large Range of Reynolds Number, Nuclear Eng. & Design, vol. 83, pp. 31-46 (1984).

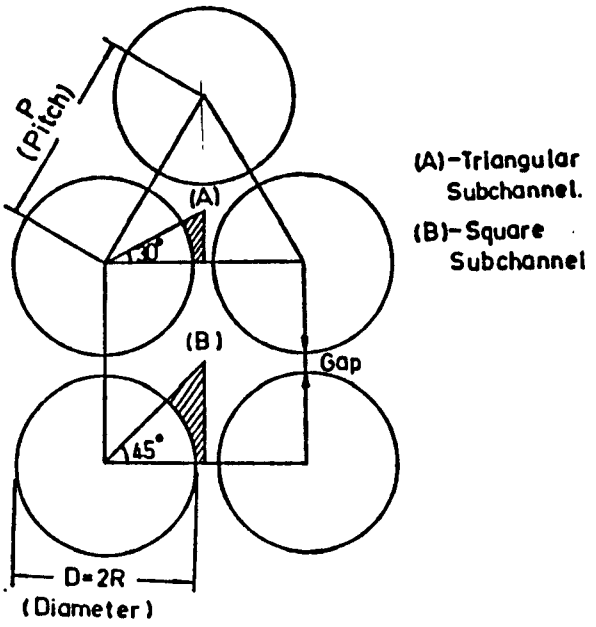

(a)

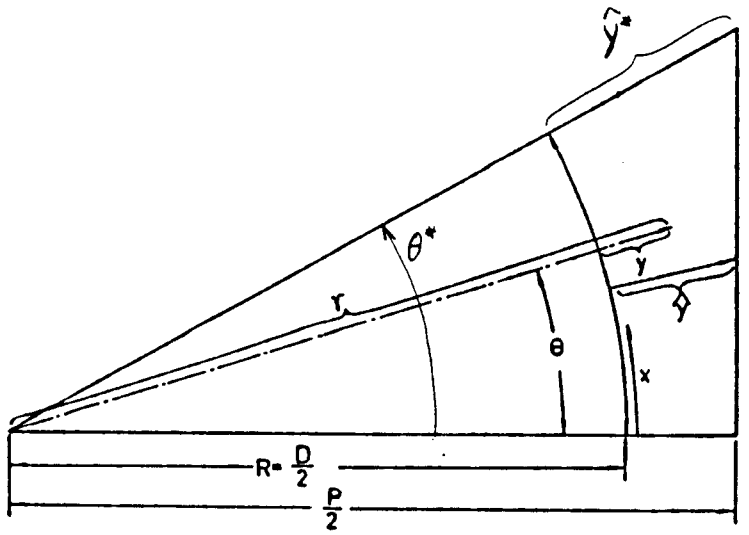

(b)

Fig. 1. (a) Subchannel for Triangular and Square Rod Arrays;

(b) Notation of Coordinates

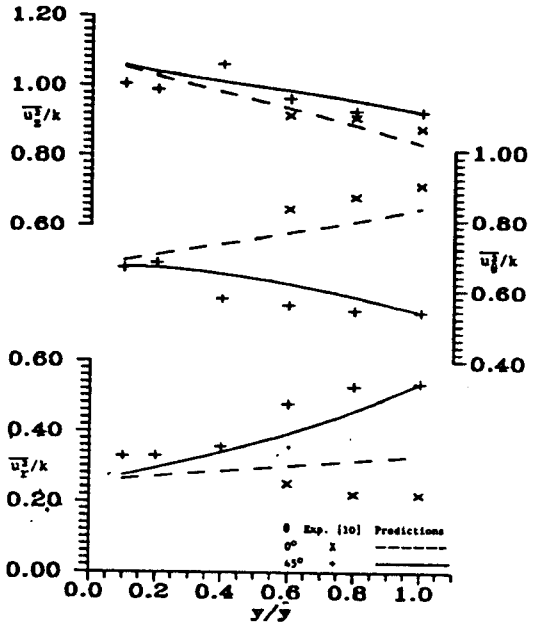

Fig.2 – Predictions for Normal Stresses, P/D = 1.107

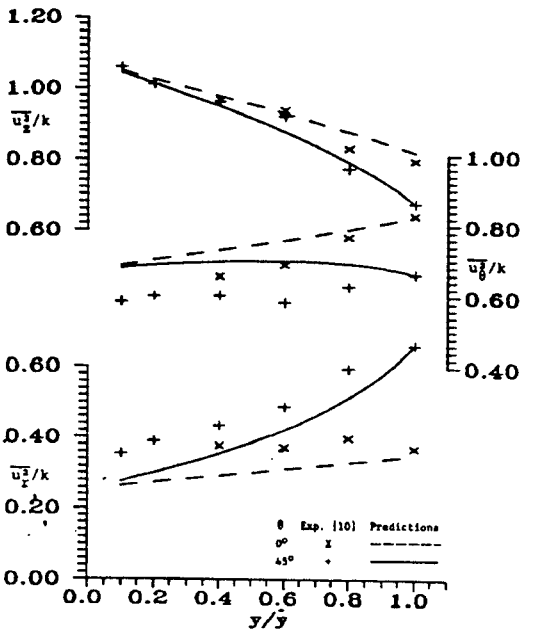

Fig.3 – Predictions for Normal Stresses, P/D = 1.194

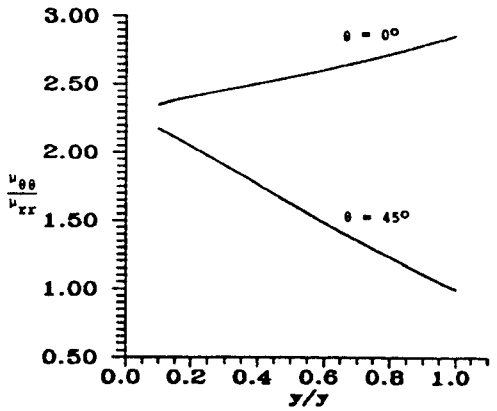

Fig.4 – Predictions for eddy diffusivity ratio
P/D = 1.107